Journal of Fluids and Structures (1997) **11,** 665–691

COMPUTATION OF NON-STATIONARY SHOCK-WAVE/CYLINDER INTERACTION USING ADAPTIVE-GRID METHODS

D. DRIKAKIS, D. OFENGEIM

UMIST, Department of Mechanical Engineering, PO Box 88, Manchester M60 1QD, U.K.

E. TIMOFEEV

Ioffe Physical-Technical Institute, Russian Academy of Sciences, Polytekhnicheskaya 26, St. Petersburg 194021, Russia

AND

P. VOIONOVICH

Advanced Technology Center, P.O. Box 29, St. Petersburg, Russia

(Received 4 June 1996 and in revised form 9 June 1997)

A numerical study of shock wave propagation over a cylinder is presented. Hybrid, structured-unstructured adaptive grids are employed for the numerical solution of the Euler and Navier-Stokes equations. A second-order Godunov-type scheme is employed for the discretization of the inviscid fluxes, while central differences are used for the viscous terms. The time integration is obtained by a second-order prediction-corrector scheme. Simulation of the unsteady gasdynamic phenomena around the cylinder is obtained at different incident-shock Mach numbers. The shock-wave diffraction over the cylinder is investigated by means of various contour plots, as well as pressure and skin friction distributions. The calculations reveal that the Euler solutions are very close to the Navier-Stokes ones in the first half of the cylinder, but large differences between the two solutions exist in the second half of the cylinder and the wake of the flow field, where strong viscous-inviscid interaction occurs.

1. INTRODUCTION

INTERACTION OF SHOCK WAVES WITH OBSTACLES has attracted the interest of many theoretical, numerical and experimental studies. This interest is largely motivated by the understanding of the physics of non-stationary gas-dynamic phenomena, as well as from the fact that oblique reflection and diffraction appear in explosion dynamics (Glass & Sislian 1994). The gas-dynamic phenomena may include several types of non-stationary interactions such as shock-obstacle, shock-shock and viscous-inviscid interactions.

0889–9746/97/060665 + 28 $25.00/fl970104

Whitham (1957) has developed an approximate theory for the dynamics of shock waves and applied this theory to the description of shock diffraction on wedges and corners. Bryson & Gross (1961) extended Whitham's theory to two- and three-dimensional bodies such as cylinders and spheres. They also performed shock tube experiments to check the accuracy of the theory and to illustrate the diffraction flow patterns. Their theoretical predictions were in very good agreement with the experimental data. Similar studies were also performed by Heilig (1960), Syshchikova *et al.* (1967), Takayama & Kawauchi (1979), Takayama & Ito (1985). An interferometric investigation of a planar shock wave over a semi-circular cylinder was also presented by Kaca (1988).

On the other hand, due to the recent advancements of Computational Fluid Dynamics (CFD), especially in the field of shock-capturing schemes and unstructured adaptive grids, very accurate simulation of non-stationary gas-dynamic phenomena can be achieved. Regarding the numerical algorithm development, the simulation of shock propagation and unsteady interaction with structures pose significantly greater demands than those required by traditional shock capturing schemes [e.g., Harten 1983], which are only intended to produce steady, non-oscillatory shocks. Past simulations of shock-wave propagation over long distances relied on either a fixed-mesh structured grid approach (Glaz *et al.* 1985) or sliding refined zones, intended to surround the shocks continuously with a finer mesh than elsewhere in the domain (Berger & Oliger 1984). Baum & Löhner (1994) carried out inviscid simulation of shock propagation over a box suspended above a rigid elevated surface. They used unstructured grids in conjunction with finite-element methods and high-resolution monotonicity-preserving algorithms (Löhner *et al.* 1988; Löhner 1987). Inviscid simulation of complicated flow fields involving strong shock waves has been presented by Woodward & Colella (1984), Colella & Glaz (1985), as well as by Glaz *et al.* (1985). Yang *et al.* (1987) studied the non-stationary shock-wave reflection generated by a blast shock wave impinging on a circular cylinder. They used structured grids and a second-order hybrid upwind method to solve the compressible Euler equations. Yang *et al.* (1993) studied shock wave reflection over a circular cylinder in a dusty gas. Their simulation was based on the two-phase Euler equations, unstructured grids, and a second-order Godunov-type scheme. Drikakis & Tsangaris (1993) have also developed high-order upwind schemes for the simulation of both inviscid and viscous flows with strong shock waves over bluff bodies including real gas effects. Ofengeim *et al.* (1993) have studied, on the basis of Euler equations, the pressure load on the cylinder surface during the diffraction of strong shock waves, while Glass *et al.* (1989) have provided direct comparison of structured-grid inviscid calculations to experiments for the cases of half-diamond and semi-circular cylinders. All the foregoing studies were focused on either the validation of the Euler unstructured-grid algorithms or the investigation of shock-wave phenomena at certain Mach numbers on the basis of *inviscid* simulation.

The aim of the present paper is to study the propagation of shock waves over a cylinder using both the Euler and Navier-Stokes equations, and more specifically to examine the viscous effects at various Mach numbers by comparing the inviscid and viscous calculations. The emphasis of the paper is on the results rather than the algorithms employed, and therefore the presentation and validation of the algorithm is kept to a sufficient, but not exhaustive, depth. In Section 2 the numerical method is described, while in Section 3 the results from the numerical study are presented. Finally, in Section 4 conclusions from the present research are drawn.

2. MATHEMATICAL MODELLING

2.1. Governing Equations

The numerical method employed has been presented in a very brief form by Beryozkina *et al.* (1996). In this paper a preliminary validation of the method was presented. A detailed description of the method is given below.

The governing equations are the two-dimensional Navier-Stokes equations, which are written in an integral form as follows:

$$\frac{\partial}{\partial t}\oint_{\Omega} \mathbf{U}\, \mathrm{d}\Omega + \oint_{S} ((\mathbf{F}_x^c + \mathbf{F}_x^v)n_x\, \mathrm{d}S + (\mathbf{F}_y^c + \mathbf{F}_y^v)n_y\, \mathrm{d}S) = \mathbf{0} \tag{1}$$

where

$$\mathbf{U} = \begin{Bmatrix} \rho \\ \rho u_x \\ \rho u_y \\ e \end{Bmatrix}, \qquad \mathbf{F}_x^c = \begin{Bmatrix} \rho u_x \\ \rho u_x^2 + p \\ \rho u_y u_x \\ (e+p)u_x \end{Bmatrix}, \qquad \mathbf{F}_y^c = \begin{Bmatrix} \rho u_y \\ \rho u_x u_y \\ \rho u_y^2 + p \\ (e+p)u_y \end{Bmatrix},$$

$$\mathbf{F}_x^v = \begin{Bmatrix} 0 \\ \tau_{xx} \\ \tau_{yx} \\ \tau_{xx}u_x + \tau_{yx}u_y + k(\partial T/\partial x) \end{Bmatrix}, \qquad \mathbf{F}_y^v = \begin{Bmatrix} 0 \\ \tau_{yx} \\ \tau_{yy} \\ \tau_{yx}u_x + \tau_{yy}u_y + k(\partial T/\partial y) \end{Bmatrix}$$

where $\mathbf{u} = (u_x, u_y)$ is the velocity vector, while p, ρ, T and e are the pressure, density, temperature and total energy, respectively. The shear stress components are represented by τ_{xx}, τ_{yx} and τ_{yy}, while $k = \mu C_p/\mathrm{Pr}$ is the heat conductivity coefficient (C_p and Pr are the specific heat at constant pressure and Prandtl number, respectively). The viscosity coefficient μ is calculated by the Sutherland's law. Ω represents a control volume bounded by the surface S, while $\mathbf{n} = (n_x, n_y)$ is the unit normal vector [Figure 1(a)].

2.2. Numerical Method

The numerical method used here is the extension of the algorithm developed by Fursenko *et al.* (1995) to simulate unsteady inviscid flows using adaptive unstructured grids. Preliminary validation of the method in viscous flows was performed by Beryozkina *et al.* (1996). In the present work the viscous flow solver is extensively validated and subsequently used for the study of shock-wave propagation phenomena over a cylinder. The main goal of the paper is the investigation of the flow phenomena rather than the algorithmic issues, but a description of the method is given below.

In viscous flows the implementation of unstructured grids in the near wall region results in very elongated triangles, which lead to a significant reduction of the CFL number. It has been found that the use of a structured grid in the near-wall region facilitates the implementation of implicit schemes which subsequently improve the efficiency of the numerical solution in the boundary layer region (Beryozkina *et al.* 1996). Therefore, in the present work a hybrid structured-unstructured grid was implemented. A structured grid (quadrilateral elements) covers a region around the solid surface, while an adaptive unstructured grid based on triangular elements covers the rest of the domain [Figure 1(b)]. A geometric rule has been used in order to define

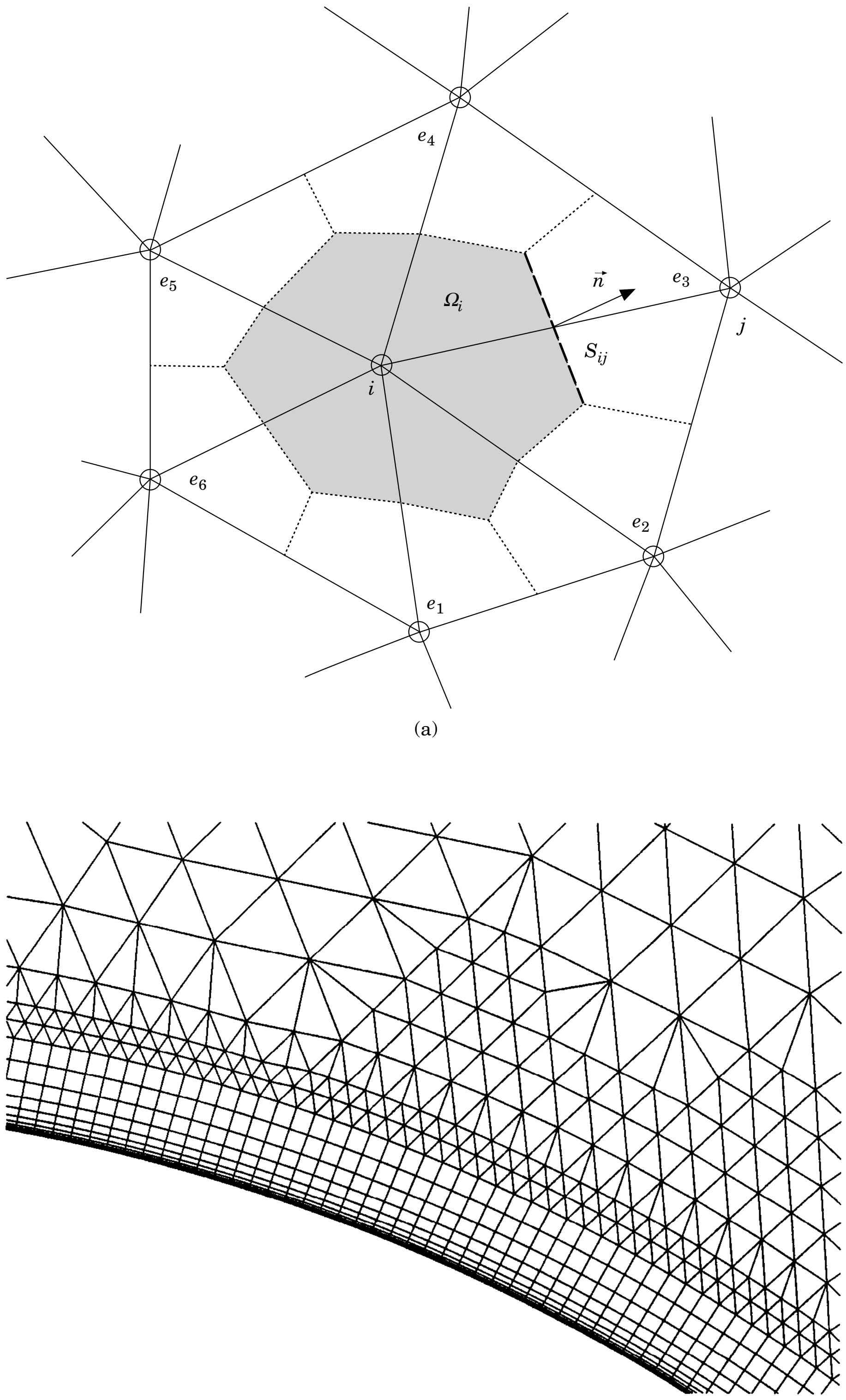

Figure 1. (a) Schematic representation of a control volume. (b) Structured-unstructured grid interface near the solid surface.

the thickness of the structured layer in the near-wall region: the size of control volumes in the region of the structured-unstructured grid interface should be almost the same, while between the structured and unstructured grid regions there are no overlapping control volumes.

2.2.1. *Unstructured grid region*

In the unstructured grid region a predictor-corrector scheme is applied for both the inviscid and viscous fluxes. In the predictor step no Riemann solver is employed, while the Roe scheme (Roe 1981) is used in the corrector step. According to Fursenko *et al.* (1995), in order to enhance the spatial accuracy a linear reconstruction of the primitive variables, $V = (\rho, u, v, p)^{\mathrm{T}}$, is used for all control volumes. The gradient $\partial V/\partial\alpha_i$ of the primitive variables on each control volume [Figure 1(a)] are calculated by the minimum value of the average gradient $\overline{\partial V}/\partial\alpha_i$ and the gradients $\partial V/\partial\alpha_e$ in the triangles (e) surrounding the node i:

$$\frac{\partial V}{\partial\alpha_i} = \min_e\left[\frac{\overline{\partial V}}{\partial\alpha_i}, 2\frac{\partial V}{\partial\alpha_e}\right], \qquad \alpha = x,y; \qquad \left(\frac{\overline{\partial V}}{\partial\alpha_i}\right) = \frac{1}{\Omega_i}\sum_e (\nabla V)_e\Omega_e \tag{2}$$

Using the above gradients, the primitive variables at the cell faces of the control volume are calculated as

$$V_{ij}^{\mathrm{in}} = V_i + 0{\cdot}5(\nabla V)_i \cdot (\overrightarrow{\mathbf{ij}}) \tag{3}$$

where $(\overrightarrow{\mathbf{ij}})$ is the vector between the nodes i and j. The predictor step calculates an intermediate value $\tilde{U}_i$ of the conservative variables as

$$\tilde{U}_i\Omega_i = U_i^n\Omega_i - \Delta t\sum_j \{[F_x^c(V_{ij}^{\mathrm{in}}) + F_x^v(V_{ij}^{\mathrm{in}})]n_xS_{ij} + [F_y^c(V_{ij}^{\mathrm{in}}) + F_y^v(V_{iy}^{\mathrm{in}})]n_yS_{ij}\} \tag{4}$$

where j denotes grid points surrounding the node i. Ω_i is the control volume around the node i and S_{ij} is the area of the interface between the volumes i and j [Figure 1(a)].

Then for each volume i the corrector step is performed:

$$U_i^{n+1}\Omega_i = U_i^n\Omega_i - \Delta t\sum_j \{[F_x^c(W_{ij}) + F_x^v(W_{ij})]n_xS_{ij} + [F_y^c(W_{ij}) + F_y^v(W_{ij})]n_yS_{ij}\} \tag{5}$$

where W_{ij} is the average value of the primitive variables obtained by the Roe scheme, considering that the left ($\tilde{V}_{ij}^{\mathrm{in}}$) and right ($\tilde{V}_{ij}^{\mathrm{out}}$) states of the Riemann problem are defined as

$$\tilde{V}_{ij}^{\mathrm{in}} = 0{\cdot}5[\tilde{V}_i + V_i + (\nabla V)_i \cdot (\overrightarrow{\mathbf{ij}})], \qquad \tilde{V}_{ij}^{\mathrm{out}} = 0{\cdot}5[\tilde{V}_j + V_j + (\nabla V)_j \cdot (\overrightarrow{\mathbf{ji}})] \tag{6}$$

The above predictor-corrector procedure (henceforth labelled as the $L(\Delta t)$ operator) is performed twice.

2.2.2. *Structured grid region*

In the structured grid region a more complicated procedure is followed in order to improve the efficiency of the unsteady calculations in the boundary layer and avoid significant reduction of the CFL number in the near-wall region. The above predictor-corrector scheme, $L(\Delta t)$, is also applied to the inviscid fluxes in the tangential to the body direction using a time step Δt (always smaller or equal to the physical one) defined as

$$\Delta t = \min(\Delta t_1, \Delta t_2) \tag{7}$$

where Δt_1 and Δt_2 are defined by

$$\Delta t_1 = \frac{\text{CFL}}{\sqrt{2}} \frac{\Delta I}{(|\mathbf{v}| + c)\left(1 + 2\dfrac{\rho \Delta l(|\mathbf{v}| + c)}{\mu \max(1, \gamma/\text{Pr})\text{Re}}\right)} \tag{8}$$

$$\Delta t_2 = \frac{\text{CFL} \cdot \Delta l}{|\vec{v}| + c} \tag{9}$$

where Δl is a characteristic length of the cell, c is the speed of sound, γ is the ratio of specific heats and Re is the Reynolds number.

The above procedure is labelled as $L_1(\Delta t)$. The same procedure is also applied to the inviscid flux in the normal direction performing m subiterations and using a time step $\Delta t/m$. This procedure is labelled as $L_2(\Delta t/m)$.

For the viscous fluxes the predictor-corrector procedure, labelled as $L^v(\Delta t)$, is written as follows:

- Predictor

$$U_{i,j}^{n+1/2} = U_{i,j}^n - \frac{\Delta t}{\Omega_{i,j}} \sum F_{(v),o}^n \tag{10}$$

- Corrector

$$U_{i,j}^{n+1} = U_{i,j}^n - 0{\cdot}5 \frac{\Delta t}{\Omega_{i,j}} \left[\sum F_{(v),o}^n + \sum F_{(v),0}^{n+1/2}\right] - 0{\cdot}5 \frac{\Delta t}{\Omega_{i,j}} \left[\sum F_{(v),m}^n + \sum F_{(v),m}^{n+1}\right] \tag{11}$$

where the sum is obtained for all faces of the quadrilateral elements. The viscous flux $F_{(v),m}$ contains the second order derivatives in the normal direction, and the flux $F_{(v),o}$ contains the rest of the viscous terms. The development of equation (11) results in a block tridiagonal matrix of coefficients, which is solved by the Thomas algorithm. The predictor-corrector procedure described above for the structured grid region is performed twice at each time step. By making use of the symbolic operators $L_1(\Delta t)$, $L_2(\Delta t/m)$ and $L^v(\Delta t)$ this procedure is represented as

$$L(\Delta t) = L_1^c(\Delta t)\left[L_2^c\left(\frac{\Delta t}{m}\right)\right]^m L^v(\Delta t) \times L^v(\Delta t)\left[L_2^c\left(\frac{\Delta t}{m}\right)\right]^m L_1^c(\Delta t) \tag{12}$$

2.3. Grid Adaptation

The local adaptation of the unstructured grid during the numerical solution provides a powerful tool for the accurate simulation of non-stationary, gas-dynamic phenomena. The adaptation algorithm in the present paper is similar to that developed by Löhner (1987). The refinement/coarsening criterion is based on second-order differences of density (Fursenko *et al.* 1995):

$$E_i = \max_e \left(\frac{|(\nabla\rho)_e - \overline{(\nabla\rho)_i}|}{|(\nabla\rho)_e| + |\overline{(\nabla\rho)_i}| + \varepsilon\,|\rho_i|\,d^{-1}}\right) \tag{13}$$

where e denotes the neighbouring triangles of the node i [Figure 1(a)]. The parameter d represents a characteristic size of the cell, and ε is a filter coefficient which has to be properly chosen to enhance grid adaptation. The grid is coarsened or refined by comparing the value of E_i at each node with the coarsening (T_c) and refining (T_r) criteria which are prescribed as input values in the computational code. If $E_i > T_r$, all triangles of vertex i will be refined, while if $E_i < T_c$ the node i may be removed.